frontiers in Earth Science

ORIGINAL RESEARCH
published: 16 April 2021
doi: 10.3389/feart.2021.662586

Quantitative Measurement of Retained Oil in Organic-Rich Shale—A Case Study on the Chang 7 Member in the Ordos Basin, China

Lianhua Hou[1], Xia Luo[1], Senhu Lin[1], Zhongying Zhao[1] and Yong Li[2]*

[1] Research Institute of Petroleum Exploration & Development, PetroChina, Beijing, China, [2] State Key Laboratory of Organic Geochemistry, Guangzhou Institute of Geochemistry, Chinese Academy of Sciences, Guangzhou, China

This study proposes a method to calculate the retained oil content (W_O) in cores collected by a sealed tool from organic-rich shale with thermal maturity around%Ro = 0.8 in the Ordos Basin, China. Approaches such as soaking cores at low temperature, multiple extractions, multiple pyrolysis, and multiple chromatographic analyses were conducted and then the relationships between total retained oil content and mineral compositions were analyzed. The total retained oil content measured by the method proposed in this paper is 60–260% higher than that measured by a conventional pyrolysis method and 34–69% higher than the sum (W_O) of two extractions with dichloromethane (W_{O3}) and chloroform (W_{O4}). After extractions with dichloromethane and chloroform (W_{O5}), the oil retained in the organic-rich shale was 4.7–11.6%, which has not been extracted. Positive correlations exist between W_O (i.e., $W_{O3} + W_{O4}$) and total organic carbon (TOC) and S_1 (absorbed hydrocarbon by rock pyrolysis), and W_O has the highest correlation coefficient with the former. The method can provide important guidance for the objective analysis of retained oil in organic-rich shale, and it is reliable for the evaluation of shale oil reserves.

Keywords: organic-rich shale, retained oil, oil content calculation, pyrolysis, sealed coring

OPEN ACCESS

Edited by:
Dongdong Wang, Shandong University of Science and Technology, China

Reviewed by:
Wenxue Han, Shandong University of Science and Technology, China
Weijiao Ma, China University of Petroleum (Huadong), China

****Correspondence:***
Lianhua Hou
houlh@petrochina.com.cn

Specialty section:
This article was submitted to Economic Geology, a section of the journal Frontiers in Earth Science

Received: *01 February 2021*
Accepted: *25 February 2021*
Published: *16 April 2021*

Citation:
Hou L, Luo X, Lin S, Zhao Z and Li Y (2021) Quantitative Measurement of Retained Oil in Organic-Rich Shale—A Case Study on the Chang 7 Member in the Ordos Basin, China. Front. Earth Sci. 9:662586. doi: 10.3389/feart.2021.662586

INTRODUCTION

Since the groundbreaking progress made by the United States on shale oil in Bakken reserves in the 1950s, technology related to shale oil in the US has been developing rapidly and achieved its profitability in 2018 (Soeder, 2018; Hackley et al., 2020; Solarin et al., 2020; Ulrich-Schad et al., 2020). Drawing lessons from the experience of the USA's shale oil development, China began to explore the technology and practice on shale oil exploration and development and made a step forward on fields including geological theory, exploration and development technology, and experimental techniques (Hou et al., 2020; Hou et al., 2021a; Kang et al., 2020; Ma et al., 2020a; Ma et al., 2020b; Zhao et al., 2020a; Zhu et al., 2021). However, more researches are needed to tackle problems related to the quantitative evaluation of the total retained oil content, the occurrence mechanism of shale oil, and pores and fluid flowing mechanism in shale formation. Among these topics, objective quantitative evaluation on the retained oil content of organic-rich shale has always been the focus of ongoing researches (Jarvie, 2012; Chen and Jiang, 2016; Abrams et al., 2017; Jiang et al., 2017; Li M. W. et al., 2019).

There are two methods commonly used to measure the total retained oil in organic-rich shale: one is conventional chloroform bitumen "A" and the other is rock pyrolysis (Stroup, 1987; Johannes et al., 2007; Han et al., 2015; Nady and Hammad, 2015; Li J. B. et al., 2019). Because light hydrocarbon is easily lost, part of the hydrocarbons in S_1 is regarded as residual hydrocarbon. Besides, conventional chloroform bitumen "A" can hardly reveal whether the shale oil is free or absorbed. The other method is modified pyrolysis (Zink et al., 2016; Chen et al., 2017; Li et al., 2018; Li M. W. et al., 2019; Ma et al., 2019; Hou et al., 2021b). In conventional source rock pyrolysis, S_1 represents the residual hydrocarbon in rock, which is the oil that has already existed, and S_2 represents the hydrocarbon potential in kerogen. In shale oil evaluation, since S_1 has compositions similar to shale oil, they can be easily extracted by dichloromethane with weak polarity. Therefore, they are treated as free shale oil. However, S_1 does not represent all free shale oil and S_2 does not completely show the hydrocarbon potential in kerogen (Chen et al., 2018; Li et al., 2018; Li M. W. et al., 2019; Ma et al., 2019; Hou et al., 2020). S_2 contains small amounts of free oil and absorbed oil, so the pyrolysis method cannot estimate the content of absorbed shale oil.

The modified method requires instantly freezing cores by liquid nitrogen in the field (at −50°C) and then crushing them in a closed system (190°C). Pyrolysis analysis immediately follows. A light hydrocarbon restoring coefficient is estimated by forward modeling, and correction to the historical data of the shale with medium–high maturity is conducted. Absorbed oil can be separated from the already generated hydrocarbon oil by changing the heating rate. But this method still shows limitations in the following aspects: firstly, online analysis cannot be achieved as crushed samples enter the pyrolysis apparatus, resulting in a partial loss of light hydrocarbon. Secondly, the assumption that kerogen generates hydrocarbon at above 300°C lacks a reliable scientific proof. Besides, since there are only a few samples (in total 100 mg), a big error may exist. For shale with abundant organic matter [total organic carbon (TOC) as high as 20–30% and hydrocarbon potential up to 100 mg/g rock], the error is noticeably high (the maximum S_2 of a standard sample in China is 16.98 mg/g rock).

SAMPLES AND METHODS

Eleven samples from Well L85 drilled in the Chang 7 member in the Ordos Basin were collected (see basic geochemical information listed in **Table 1**). After taken into a sealed tool, the cores were wiped with cotton to remove the sealing fluid on their surface within 1.5 h so that they will not be eroded by the sealing fluid. Then, the cores are weighed and put into containers filled with dichloromethane solution. The cores should be completely submerged into the solution by at least 2 cm below. Finally, the containers (i.e., sealed bottles) containing the dichloromethane solution and cores were put into a freezer where the temperature remained below 20°C to prevent the dichloromethane solution from evaporating (the boiling point of dichloromethane is 39.5°C). After all these were done, the samples were moved from the field to the laboratory.

After immersing the cores for 10–30 days, 5 ml of methylbenzene was added to the bottle as the standard sample. The solution was placed into a crusher and then the crusher put into liquid nitrogen. The core sample was crushed into particles of 0.18 mm. The crushed sample and the dichloromethane were moved into a bottle and sealed with a cap, and then chromatographic analysis was immediately started (the above procedure is denoted as step 1). After being immersed for 10–30 days, the core sample was separated from the solution. The solution was measured and then 1 ml solution was taken and put into two flasks (labeled A and B) marked with internal rulers. Quantitative analysis of total hydrocarbon gas chromatography in a flask (A#) was conducted (the above procedure is denoted as step 2). Into another flask (B#), after full evaporation, solvent was add to 1 ml and then chromatographic analysis was conducted (the above procedure is denoted as step 3). The rest of solution was weighed after full evaporation. The rest of the crushed sample was placed into the dichloromethane solution after weighing and extraction. Of the solution, 1 ml was taken after the isochoric process and put into two flasks (labeled C and D) with internal rulers. Quantitative analysis of total hydrocarbon gas chromatography in a flask (C#) was conducted (the above procedure is denoted as step 4). Another flask (D#), after full evaporation, is added with solvent to 1 ml and then chromatographic analysis was started (the above procedure is denoted as step 5). The remaining solution was weighed after full evaporation. A certain amount of the sample powder was take after drying, weighed, and the pyrolysis analysis conducted (the above procedure is denoted as REP 1; the results are listed in **Table 2**). The remaining sample powder was placed into a chloroform solution after weighing and extraction. The solution was completely evaporated and weighed. Again, a certain amount of dried sample was weighed and rock pyrolysis was conducted (the above procedure is denoted as REP 2). The experiments above were conducted at the National Key Laboratory of Enhanced Oil Recovery, Research Institute of Petroleum Exploration & Development, PetroChina.

RESULTS AND DISCUSSION

Chromatographic Analysis

Figures 1–5 show the chromatographic analysis of the core samples that went through the above steps 1–5. Taking sample 6 as an example, the calculation process is given in **Appendix Table A1**. The samples have been completely immersed in dichloromethane solution for 10–30 days before being crushed in liquid nitrogen, and then followed by immediate gas chromatography analysis (**Figure 1**). The light components remain intact, and a complete series of light hydrocarbons, namely, nC_5, nC_6, nC_7, nC_8, and nC_9, can be detected. The peak area of nC_7 is the largest, and nC_9 is the main peak. The powder was separated from the solution after the sample was crushed and immersed for 10–30 days. After the isochoric process, 1 ml of the solution was added into flasks A and B with internal rulers.

TABLE 1 | Basic geochemical data of the experiment samples.

Sample no.	Depth (m)	TOC (%)	Quartz (%)	Potash feldspar (%)	Plagioclase (%)	Calcite (%)	Dolomite (%)	Siderite (%)	Pyrite (%)	Clay (%)
1	1,576.86	6.34	23.4	1.0	7.9	0.0	12.1	0.0	12.4	43.2
2	1,579.86	32.842	21.6	5.7	4.6	0.0	2.4	0.0	35.9	29.8
3	1,580.34	6.63	20.0	3.4	5.1	3.3	7.5	12.1	9.7	38.9
4	1,581.07	20.87	16.7	4.3	7.1	0.0	7.1	0.0	36.3	28.5
5	1,581.91	25.77	29.9	1.8	1.8	0.0	1.6	0.0	31.3	33.6
6	1,583.47	37.86	23.6	2.5	1.0	0.0	5.7	0.0	32.8	34.4
7	1,584.91	18.6	30.9	6.0	3.3	4.2	3.6	0.0	42.0	10.0
8	1,586.23	18.83	37.8	2.5	6.1	0.0	0.9	0.0	40.6	12.1
9	1,589.85	13.09	29.9	1.5	6.2	0.8	1.9	0	15.5	44.4
10	1,591.89	12.83	25.4	1.5	5.8	0.4	1.0	0.0	10.1	22.0
11	1,592.25	18.67	26.1	3.1	4.0	4.9	6.4	0.0	35.7	19.8

TOC, total organic carbon.

TABLE 2 | Pyrolysis results of samples after various treatments.

sample no.	depth (m)	s_{01} (mg/g)	s_{02} (mg/g)	t_{max0} (°C)	s_{11} (mg/g)	s_{12} (mg/g)	t_{max1} (°C)	s_{21} (mg/g)	s_{22} (mg/g)	t_{max2} (°C)
1	1,576.86	3.75	15.66	440	0.24	12.80	439	0.17	10.23	441
2	1,579.86	7.39	149.38	439	0.74	137.96	437	0.60	129.70	436
3	1,580.34	5.39	30.77	443	0.19	13.83	441	0.15	13.47	444
4	1,581.07	10.05	87.20	442	0.86	82.84	442	0.55	79.71	441
5	1,581.91	8.19	105.41	438	1.06	95.40	436	0.67	91.93	439
6	1,583.47	13.33	150.92	440	0.77	137.57	440	0.66	132.20	442
7	1,584.91	9.89	70.54	441	1.50	57.73	439	0.61	51.34	442
8	1,586.23	5.25	79.98	441	0.89	61.14	442	0.57	57.64	442
9	1,589.85	4.07	95.89	440	0.93	87.99	439	0.68	82.75	440
10	1,591.89	4.21	70.88	441	0.69	64.29	437	0.61	60.06	436
11	1,592.25	5.51	64.86	439	0.49	55.61	439	0.38	46.47	436

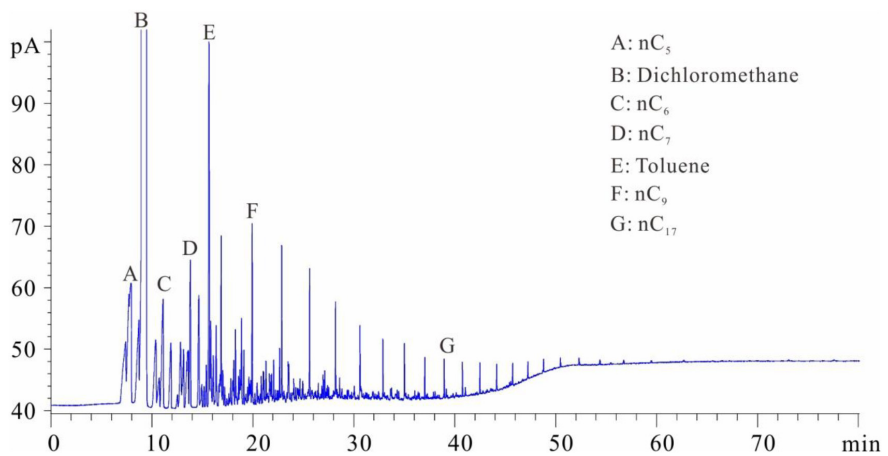

FIGURE 1 | Chromatogram of samples that were soaked first and then crushed (chromatogram after step 1).

Quantitative analysis of total hydrocarbon gas chromatography was directly conducted for flask A (see the result in **Figure 2**). Light hydrocarbons are lost as the immersion time increases (**Figure 2**). Among them, all of C_5 is lost, and the losses of nC_6 and nC_7 are 52.58 and 26.64%, respectively. C_8 and later hydrocarbons gradually increase, and W_{O1} is calculated to be 0.032 kg/t rock. In **Figure 2**, toluene and D-C_{24} standard samples are used for compound calibration. The results show that the error of the two types of standard samples for normal alkanes is 13.55%, and the calibration value of D-C_{24} is slightly higher, indicating that these two standard samples can be used. Solvent was added into flask B to 1 ml after fully evaporating and then chromatographic analysis proceeded (see the result in **Figure 3**). After the rock soaking solution volatilized completely at room

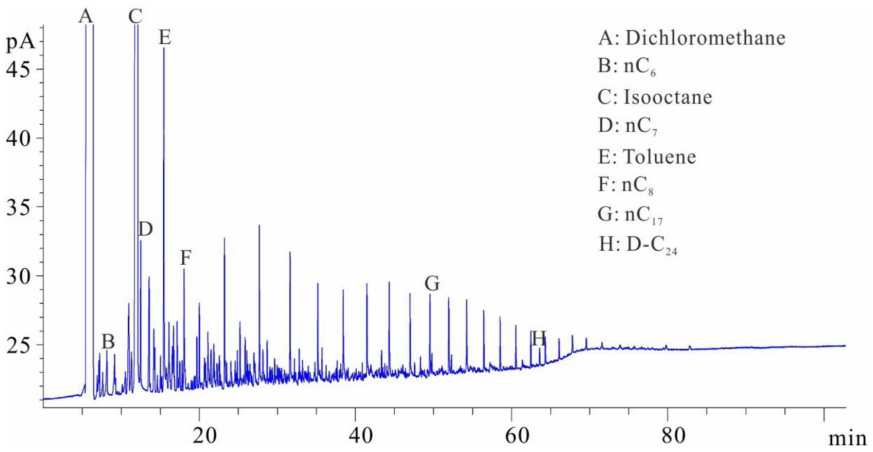

FIGURE 2 | Chromatogram of samples that were crushed first and then soaked (chromatogram after step 2).

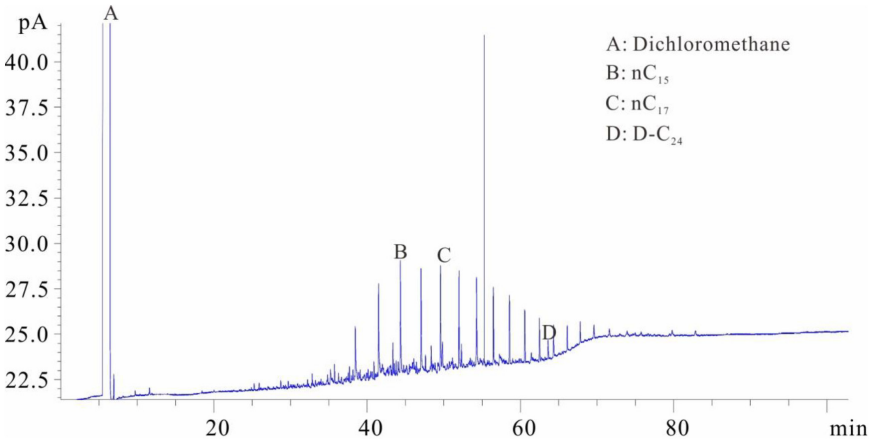

FIGURE 3 | Chromatogram of samples that were soaked first and then evaporated (chromatogram after step 3).

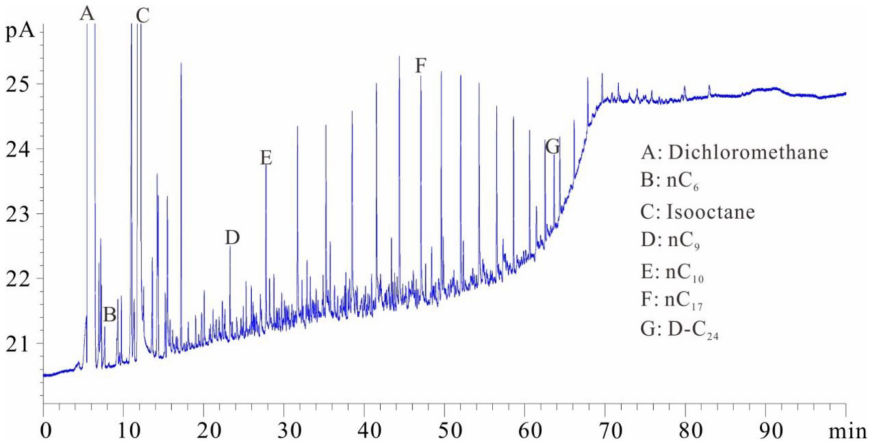

FIGURE 4 | Chromatogram of samples after dichloromethane extractions (chromatogram after step 4).

temperature, the hydrocarbons before nC_{13} are almost lost. The results show that the losses of nC_{13}, nC_{14}, and nC_{15} are 46.76, 14.57, and 0.43%, respectively. The two calculation results of nC_{16}–nC_{25} are within + 10%. Light hydrocarbons before C_{14} were quantitatively analyzed by chromatography. The pre-C_{14} hydrocarbons precipitated by sample soaking are 1.91 kg/t rock, accounting for 32.51% of the total hydrocarbons.

The samples were placed into the dichloromethane solution for extraction after separating the solution from the crushed sample. One milliliter of the extracted solution was collected and placed into flasks C and D with internal rulers after the isochoric process. Quantitative analysis of total hydrocarbon gas chromatography was directly conducted in flask C (similar to flask A) (see the result in **Figure 4**). The shales were soaked in dichloromethane and then extracted. The extraction product is divided into two parts: one part is that of hydrocarbons after C_{10} and the other part is of the isomeric hydrocarbons of C_6–C_7 (**Figure 4**). The molecular radius of this part of the hydrocarbons is small. The hydrocarbons in this part are stored in the shale nanopores and cannot be completely precipitated

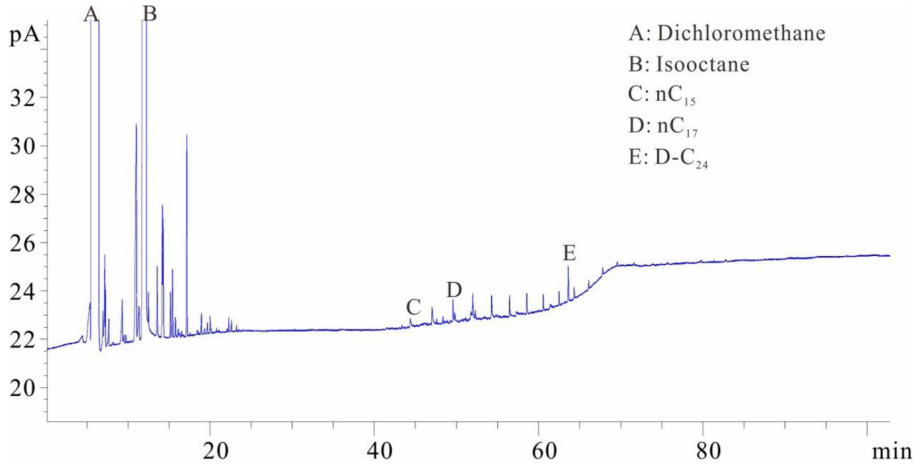

FIGURE 5 | Chromatogram of samples after chloroform extractions (chromatogram after step 5).

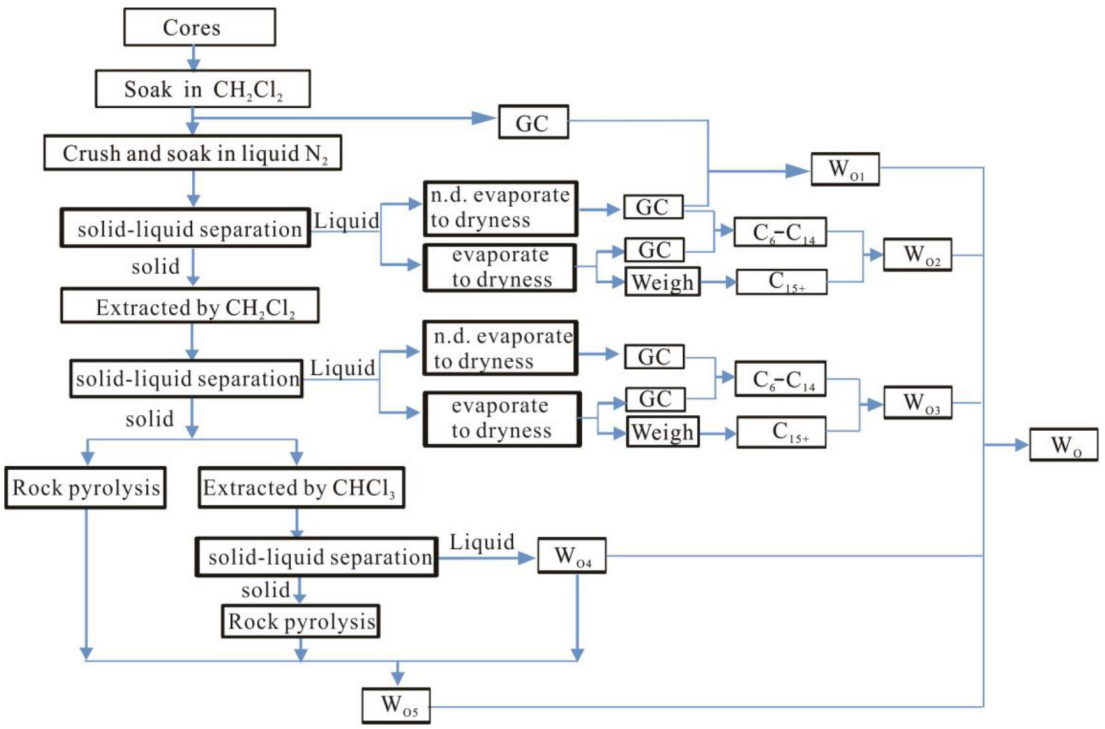

FIGURE 6 | Measuring procedures of the retained oil content in organic-rich shale.

by the dichloromethane. One milliliter solvent was added into flask D after fully evaporating and chromatographic analysis was conducted (similar to flask B) (**Figure 5**). The D volumetric flask is not easy to volatilize completely during the experiment, so the storage time is very long. Due to the long storage time, the normal alkanes before nC_{17} have all been lost. However, the C_6–C_7 isomeric alkanes in **Figure 4** are not significantly reduced in **Figure 5**. It is speculated that these C_6–C_7 isomeric alkanes may coexist with resins and asphaltenes and are extremely difficult to volatilize.

Pyrolysis Analysis

After drying the rock samples, pyrolysis analysis was immediately conducted. The results are denoted as S_{01}, S_{02}, and T_{max0} (**Table 2**). Pyrolysis analysis was conducted for the second time after the samples were extracted by dichloromethane and dried by fully evaporating (after REP 1) (Jiang et al., 2017; Li et al., 2018; Li M. W. et al., 2019; Li J. B. et al., 2019). The results are denoted as S_{11}, S_{12}, and T_{max1} (**Table 2**). After weighing, the remaining sample powder was placed in chloroform solution for extraction. Then, after chloroform evaporated, the samples were weighed and dried (after REP 2). Finally, pyrolysis experiment was done for the third time (Sun et al., 2019; Hou et al., 2020). The results are denoted as S_{21}, S_{22}, and T_{max2} (**Table 2**).

Calculations of Retained Oil Content in Organic-Rich Shale

We conducted sealed coring to organic shale that has a maturity level of%Ro = 0.8 in the Ordos Basin to calculate the total retained oil content. The core sample went through procedures including low-temperature soaking, multiple extractions, multiple pyrolysis, and multiple chromatographic analyses (refer to Section "Samples and Methods" for detailed experiment procedures). This study developed an integrated approach to measuring the total retained oil content in organic-rich shale (Chen and Jiang, 2016; Chen et al., 2018; Li et al., 2018; Li M. W. et al., 2019; Ma et al., 2019; Hou et al., 2020). The workflow is shown as follows (**Figure 6**).

The detailed calculation process is as follows:

$$W_{O1} = S_{T1} - S_{T2} \quad (1)$$

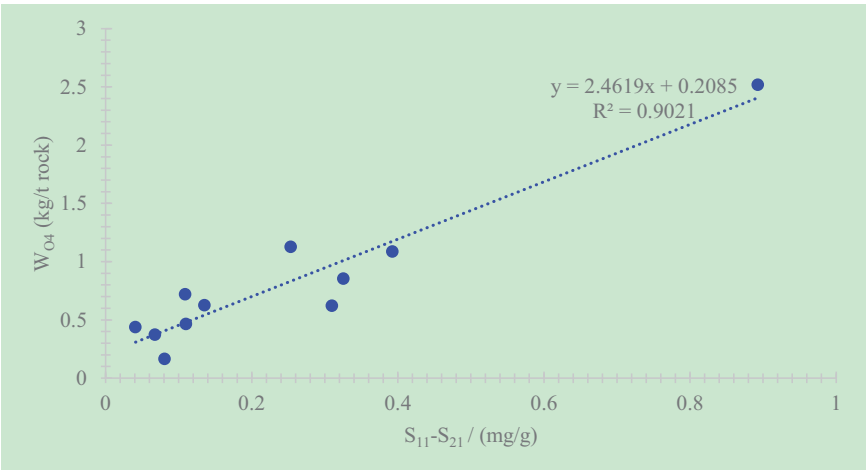

FIGURE 7 | Diagram between W_{O4} and S_{11}–S_{21}.

TABLE 3 | Calculation of oil content in organic-rich shale.

Sample no.	Depth (m)	W_{O1} (kg/t rock)	W_{O2} (kg/t rock)	W_{O3} (kg/t rock)	W_{O4} (kg/t rock)	W_{O5} (kg/t rock)	W_O (kg/t rock)
1	1576.86	0.015	1.587	3.530	0.372	0.607	6.111
2	1579.86	0.005	6.369	11.984	0.625	1.997	20.980
3	1580.34	0.089	3.557	8.861	0.438	0.632	13.577
4	1581.07	0.059	5.390	9.979	0.620	1.666	17.714
5	1581.91	0.006	4.361	15.882	1.086	2.059	23.394
6	1583.47	0.003	5.876	19.139	0.719	2.357	28.094
7	1584.91	0.092	3.458	8.631	2.518	1.925	16.624
8	1586.23	0.088	4.183	12.093	0.854	1.704	18.922
9	1589.85	0.015	2.354	7.487	1.126	0.593	11.575
10	1591.53	0.022	2.493	7.058	0.165	0.575	10.313
11	1592.25	0.009	4.502	7.861	0.464	1.236	14.072

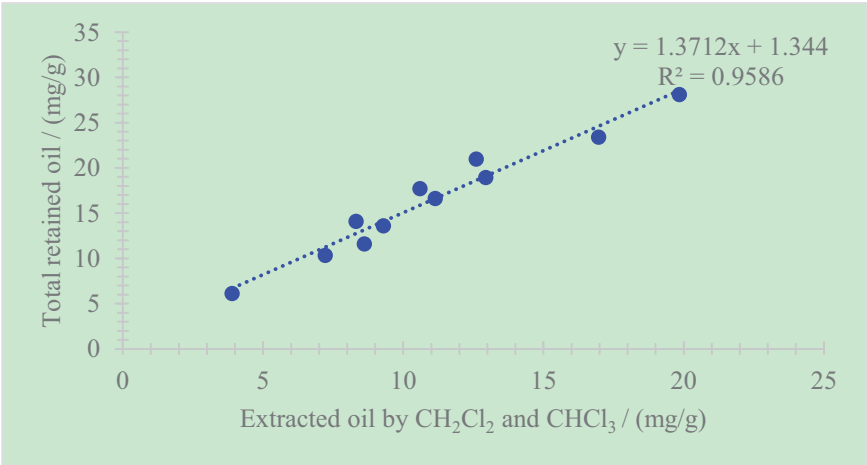

FIGURE 8 | Relationship between the total retained oil content and the extracted sum of dichloromethane and chloroform.

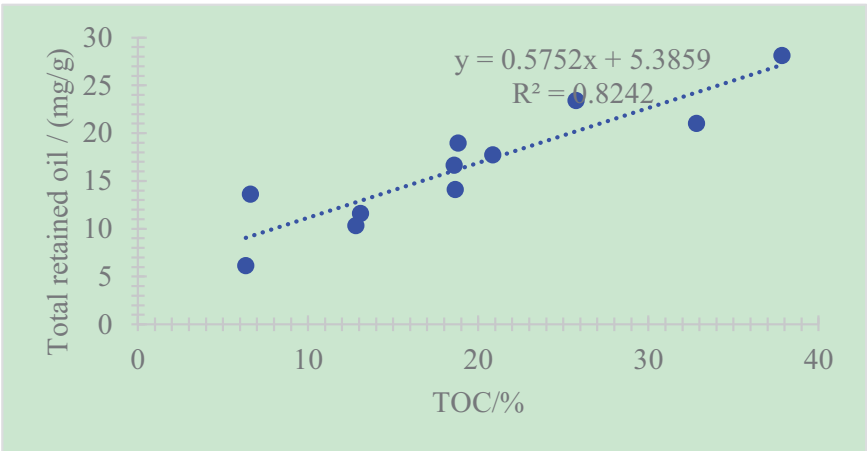

FIGURE 9 | Relationship between the total retained oil content and TOC.

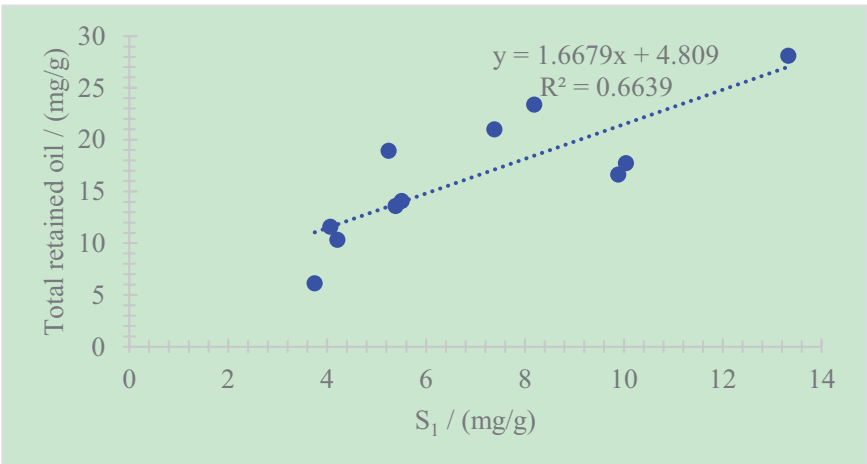

FIGURE 10 | Relationship between the total retained oil content and S_1.

W_{O1} refers to the difference (C_5–C_7) between the core samples after step 2 and after step 1 (in flask A#).

$$W_{O2} = S_{T3} - S_{T2} + W_{V1} \quad (2)$$

W_{O2} refers to the difference (C_6–C_{14}) between the core samples after step 3 (flask B#) and after step 2 (flask A#), plus the weight W_{V1} of the evaporated solution remaining after step 2. S_{T3} - S_{T2} refers to the light hydrocarbon in the sample.

$$W_{O3} = S_{T5} - S_{T4} + W_{V2} \quad (3)$$

W_{O3} represents the difference (C_6–C_{14}) between the core samples after step 5 (D#) and after step 4 (C#), plus the weight W_{V2} of the evaporated solution remaining after step 5. S_{T5} - S_{T4} refers to the light hydrocarbon in the sample.

The solution, after extracted by chloroform, filtered, and evaporated completely, is weighed to be W_{O4}. The hydrocarbons retained in the shale after chloroform extraction is defined as W_{O5}, and this part of hydrocarbons can be calculated from **Figure 7**. After the shale is extracted by dichloromethane and chloroform, the difference of the two pyrolysis S_1 values and the amount of chloroform extraction show a positive relationship. Therefore, pyrolysis analysis of the rock after chloroform extraction can infer the retained hydrocarbon content in the rock according to the S_1 content.

Therefore, the calculated oil content in shale should include five parts (**Table 3**), namely:

$$W_O = W_{O1} + W_{O2} + W_{O3} + W_{O4} + W_{O5} \quad (4)$$

The retained oil W_{O4} in organic-rich shale after extracted by dichloromethane and chloroform accounts for 4.65–11.58%. In other words, there is 4.65–11.58% of retained oil that can hardly be soluble in organic solvent in organic-rich shale, and this part of retained oil can hardly be extracted.

Correlation Analysis of Geochemical Parameters

The total retained oil content shows good correlations with the extracted sum of dichloromethane and chloroform, whose correlation coefficient is R^2 = 0.96 (**Figure 8**). This phenomenon illustrates that the primary components in the total retained oil are mainly soluble organic matter that can be extracted by dichloromethane and chloroform. In other words, the retained oil in organic-rich shale can be extracted using some techniques.

A positive correlation between the total retained oil content and TOC exists, with R^2 = 0.82 (**Figure 9**). This phenomenon demonstrates that the increase in TOC may cause more shale oil remaining in rock, namely, retained oil (Hou et al., 2020; Shao et al., 2020; Zhao et al., 2020b). To explore shale oil, shale with a higher TOC is the target.

A positive correlation exists between the total retained oil content and S_1 (Chen et al., 2017; Chen et al., 2018; Li et al., 2018; Li M. W. et al., 2019; Ma et al., 2019). The correlation coefficient is R^2 = 0.66 (**Figure 10**). The relatively weak correlation also shows that the retained oil in shale cannot be calculated objectively only by the method of conventional rock pyrolysis.

CONCLUSION

This study took sealed cores of organic-rich shale in the Ordos Basin and measured the total retained oil (W_O) *via* approaches including low-temperature soaking, multiple extractions, multiple pyrolysis, and multiple chromatographic analyses. The W_O value obtained from the new method is 60–260% higher than that obtained from conventional pyrolysis and 34–69% higher than the sum of the extractions by dichloromethane (W_{O3}) and chloroform (W_{O4}). Even after extraction by dichloromethane and chloroform, there remains 4.7–11.6% hydrocarbon retained in the organic-rich shale (W_{O5}). The total retained oil content (W_O) in the organic-rich shale exhibits a positive relationship with the sum of the extractions using dichloromethane and chloroform (W_{O3} + W_{O4}), with R^2 reaching 0.96. This indicates that the primary composition in the total retained oil is soluble organic matter and is extractable *via* dichloromethane and chloroform. Positive correlations can also be observed between W_O and TOC, and S_1 through coefficients of 0.82 and 0.66, respectively.

DATA AVAILABILITY STATEMENT

The original contributions presented in the study are included in the article/supplementary material, further inquiries can be directed to the corresponding author/s.

AUTHOR CONTRIBUTIONS

LH: conceptualization, methodology, investigation, and writing – original draft. XL: data curation, writing – review and editing. SL: formal analysis, resources. ZZ: software, validation, and project administration. YL: funding acquisition. All authors contributed to the article and approved the submitted version.

FUNDING

This study was funded by PetroChina Co., Ltd. (grant nos. 2015D-4810-02 and 2018ycq03), the Research on Exploration and Development Technology of Unconventional Oil and Gas Resources (2012A-4802-02), and the Formation Mechanism and Enrichment Regularity of Terrestrial Tight Oil (Shale Oil) in China (2014CB239000).

ACKNOWLEDGMENTS

We express our genuine appreciation to Professor Jones and Harris for their constructive comments and revisions. We also thank Dr. Johnson for his language editing and polishing work.

REFERENCES

Abrams, M. A., Gong, C. Y., Garnier, C., and Sephton, M. A. (2017). A new thermal extraction protocol to evaluate liquid rich unconventional oil in place and in-situ fluid chemistry. *Mar. Pet. Geol.* 88, 659–675. doi: 10.1016/j.marpetgeo.2017.09.014

Chen, Z. H., Guo, Q. L., Jiang, C. Q., Liu, X. J., Reyes, J., Mort, A., et al. (2017). Source rock characteristics and Rock-Eval-based hydrocarbon generation kinetic models of the lacustrine chang-7 Shale of triassic Yanchang Formation, Ordos Basin, China. *Int. J. Coal Geol.* 182, 52–65. doi: 10.1016/j.coal.2017.08.017

Chen, Z. H., and Jiang, C. Q. (2016). A revised method for organic porosity estimation in shale reservoirs using rock-eval data: example from Duvernay Formation in the western Canada sedimentary basin. *AAPG Bull.* 100, 405–422. doi: 10.1306/08261514173

Chen, Z. H., Li, M. W., Ma, X. X., Cao, T. T., Liu, X. J., Li, Z. M., et al. (2018). Generation kinetics based method for correcting effects of migrated oil on rock-eval data – an example from the eocene Qianjiang Formation, Jianghan Basin, China. *Int. J. Coal Geol.* 195, 84–101. doi: 10.1016/j.coal.2018.05.010

Hackley, P. C., Dennen, K. O., Garza, D., Lohr, C. D., Valentine, B. J., Hatcherian, J. J., et al. (2020). Oil-source rock correlation studies in the unconventional Upper Cretaceous Tuscaloosa marine shale (TMS) petroleum system, Mississippi and Louisiana, USA. *J. Pet. Sci. Eng.* 190:107015. doi: 10.1016/j.petrol.2020.107015

Han, H., Zhong, N. N., Huang, C. X., and Zhang, W. (2015). Pyrolysis kinetics of oil shale from northeast China: implications from thermogravimetric and rock–eval experiments. *Fuel* 159, 776–783. doi: 10.1016/j.fuel.2015.07.052

Hou, L. H., Luo, X., Han, W. X., Lin, S. H., Pang, Z. L., and Liu, J. Z. (2020). Geochemical evaluation of the hydrocarbon potential of shale oil and its correlation with different minerals-a case study of the TYP shale in the Songliao Basin, China. *Energy Fuels* 34, 11998–12009. doi: 10.1021/acs.energyfuels.0c01285

Hou, L. H., Ma, W. J., Luo, X., Liu, J. Z., Lin, S. H., and Zhao, Z. Y. (2021a). Hydrocarbon generation-retention-expulsion mechanism and shale oil producibility of the Permian lucaogou shale in the Junggar Basin as simulated by semi-open pyrolysis experiments. *Mar. Pet. Geol.* 125:104880. doi: 10.1016/j.marpetgeo.2020.104880

Hou, L. H., Luo, X., Zhao, Z. Y., and Zhang, L. J. (2021b). Identification of oil produced from shale and tight reservoirs in the permian lucaogou shale sequence, Jimsar Sag, Junggar Basin, NW China. *ACS Omega* 6, 2127–2142. doi: 10.1021/acsomega.0c05224

Jarvie, D. M. (2012). "Shale resource systems for oil and gas: part 1- shale-gas resource systems," in *Shale Reservoirs Giant Resources for the 21st Century*, Vol. 97, ed. J. A. Breyer (Tulsa: AAPG Memoir), 69–87.

Jiang, C. Q., Chen, Z. H., Lavoie, D., Percival, J. B., and Kabanov, P. (2017). Mineral carbon MinC (%) from Rock-Eval analysis as a reliable and cost-effective measurement of carbonate contents in shale source and reservoir rocks. *Mar. Pet. Geol.* 83, 184–194. doi: 10.1016/j.marpetgeo.2017.03.017

Johannes, I., Kruusement, K., and Veski, R. (2007). Evaluation of oil potential and pyrolysis kinetics of renewable fuel and shale samples by Rock-Eval analyzer. *J. Anal. Appl. Pyrol.* 79, 183–190. doi: 10.1016/j.jaap.2006.12.001

Kang, Z. Q., Zhao, Y. S., and Yang, D. (2020). Review of oil shale in-situ conversion technology. *Appl. Energy* 269:115121. doi: 10.1016/j.apenergy.2020.115121

Li, M. W., Chen, Z. H., Cao, T. T., Ma, X. X., Liu, X. J., Li, Z. M., et al. (2018). Expelled oils and their impacts on Rock-Eval data interpretation, Eocene Qianjiang Formation in Jianghan Basin, China. *Int. J. Coal Geol.* 191, 37–48. doi: 10.1016/j.coal.2018.03.001

Li, M. W., Chen, Z. H., Ma, X. X., Cao, T. T., Qian, M. H., Jiang, Q. G., et al. (2019). Shale oil resource potential and oil mobility characteristics of the Eocene-Oligocene Shahejie Formation, Jiyang Super-Depression, Bohai Bay Basin of China. *Int. J. Coal Geol.* 204, 130–143. doi: 10.1016/j.coal.2019.01.013

Li, J. B., Wan, M., Chen, Z. H., Lu, S. F., Jiang, C. Q., Chen, G. H., et al. (2019). Evaluating the total oil yield using a single routine Rock-Eval experiment on as-received shales. *J. Anal. Appl. Pyrol.* 144:104707. doi: 10.1016/j.jaap.2019.104707

Ma, W. J., Hou, L. H., Luo, X., Liu, J. Z., Tao, S. Z., Guan, P., et al. (2020a). Generation and expulsion process of the chang 7 oil shale in the ordos basin based on temperature-based semi-open pyrolysis: implications for in-situ conversion process. *J. Pet. Sci. Eng.* 190:107035. doi: 10.1016/j.petrol.2020.107035

Ma, W. J., Hou, L. H., Luo, X., Tao, S. Z., Guan, P., Liu, J. Z., et al. (2020b). Role of bitumen and NSOs during the decomposition process of a lacustrine Type-II kerogen in semi-open pyrolysis system. *Fuel* 259:116211. doi: 10.1016/j.fuel.2019.116211

Ma, X. X., Li, M. W., Pang, X. Q., Wei, X. Y., Qian, M. H., Tao, G. L., et al. (2019). Paradox in bulk and molecular geochemical data and implications for hydrocarbon migration in the inter-salt lacustrine shale oil reservoir, Qianjiang Formation, Jianghan Basin, central China. *Int. J. Coal Geol.* 209, 72–88. doi: 10.1016/j.coal.2019.05.005

Nady, M. M. E., and Hammad, M. M. (2015). Organic richness, kerogen types and maturity in the shales of the Dakhla and Duwi formations in Abu Tartur area, Western Desert, Egypt: implication of rock–eval pyrolysis. *Egypt. J. Pet.* 24, 423–428. doi: 10.1016/j.ejpe.2015.10.003

Shao, D. Y., Zhang, T. W., Ko, L. T., Li, Y. F., Yan, J. P., Zhang, L. L., et al. (2020). Experimental investigation of oil generation, retention, and expulsion within Type II kerogen-dominated marine shales: insights from gold-tube nonhydrous pyrolysis of Barnett and Woodford Shales using miniature core plugs. *Int. J. Coal Geol.* 217:103337. doi: 10.1016/j.coal.2019.103337

Soeder, D. J. (2018). The successful development of gas and oil resources from shales in North America. *J. Pet. Sci. Eng.* 163, 399–420. doi: 10.1016/j.petrol.2017.12.084

Solarin, S. A., Gil-Alana, L. A., and Lafuente, C. (2020). An investigation of long range reliance on shale oil and shale gas production in the U.S. market. *Energy* 195:116933. doi: 10.1016/j.energy.2020.116933

Stroup, C. H. (1987). The effect of organic matter type and organic carbon content on Rock-Eval hydrogen index in oil shales and source rocks. *Org. Geochem.* 11, 351–369. doi: 10.1016/0146-6380(87)90068-4

Sun, J., Xiao, X. M., Cheng, P., and Tian, H. (2019). Formation and evolution of nanopores in shales and its impact on retained oil during oil generation and expulsion based on pyrolysis experiments. *J. Pet. Sci. Eng.* 176, 509–520. doi: 10.1016/j.petrol.2019.01.071

Ulrich-Schad, J. D., Larson, E. C., Fernando, F., and Abulbasher, A. (2020). The Goldilocks view: support and skepticism of the impacts and pace of unconventional oil and gas development in the bakken shale of the United States. *Energy Res. Soc. Sci.* 70:101799. doi: 10.1016/j.erss.2020.101799

Zhao, W. Z., Zhu, R. K., Hu, S. Y., Hou, L. H., and Wu, S. T. (2020a). Accumulation contribution differences between lacustrine organic-rich shales and mudstones and their significance in shale oil evaluation. *Pet. Explor. Dev.* 47, 1160–1171. doi: 10.1016/s1876-3804(20)60126-x

Zhao, X. Z., Zhou, L. H., Pu, X. G., Jin, F. M., Shi, Z. N., Han, W. Z., et al. (2020b). Formation conditions and enrichment model of retained petroleum in lacustrine shale: a case study of the Paleogene in Huanghua depression, Bohai Bay Basin, China. *Pet. Explor. Dev.* 47, 916–930. doi: 10.1016/s1876-3804(20)60106-9

Zhu, J. Y., Yi, L. P., Yang, Z. Z., and Li, X. G. (2021). Numerical simulation on the in situ upgrading of oil shale reservoir under microwave heating. *Fuel* 287:119533.

Zink, K. G., Scheeder, G., Stueck, H. L., Biermann, S., and Blumenberg, M. (2016). Total shale oil inventory from an extended rock-eval approach on non-extracted and extracted source rocks from Germany. *Int. J. Coal Geol.* 163, 186–194. doi: 10.1016/j.coal.2016.06.023

Conflict of Interest: LH, XL, SL, and ZZ are employed by PetroChina Co., Ltd. The authors declare that this study received funding from PetroChina Co., Ltd. The funder was not involved in the study design, collection, analysis, interpretation of data, the writing of this article, or the decision to submit it for publication.

The remaining author declares that the research was conducted in the absence of any commercial or financial relationships that could be construed as a potential conflict of interest.

APPENDIX

TABLE A1 | Typical chromatogram table of sample 6 and the calculation process.

Hydro carbons	Peak area					Calculation process							
	Step 1	Step 2	Step 3	Step 4	Step 5	Step 1 (mg)	Step 2: toluene SS (mg)	Step 2: (D-C24 SS (mg)	Step 3 (mg)	Step 4 (mg)	Step 5 (mg)	Step 2 - Step 1	Step 3 - Step 2
*n*C5	129.234					6.851							
*n*C6	104.583	7.323		1.636		5.544	2.631	3.044		0.741		-52.540	
*n*C7	142.175	15.388		1.844		7.537	5.529	6.396		0.836		-26.640	
Toluene	245.039	36.152		19.204		12.990	12.990	15.027		8.704		0.000	
*n*C8	81.334	23.456		1.656		4.312	8.428	9.750		0.750		95.472	
*n*C9	80.899	33.309		4.488		4.289	11.968	13.845		2.034		179.075	
*n*C10	60.581	40.674		8.974		3.212	14.615	16.907		4.068		355.075	
*n*C11	52.359	36.367		11.264		2.776	13.067	15.116		5.105		370.781	
*n*C12	36.814	26.661		10.615		1.952	9.580	11.082		4.811		390.870	
*n*C13	25.254	24.416	11.724	11.062		1.339	8.773	10.149	5.40	5.014		555.311	-46.767
*n*C14	22.129	24.507	18.885	12.329		1.173	8.806	10.187	8.70	5.588		650.639	-14.570
*n*C15	20.682	29.183	26.211	14.538		1.096	10.486	12.130	12.08	6.589		856.402	-0.428
*n*C16	18.202	22.812	21.728	13.022	0.015	0.965	8.197	9.482	10.01	5.902	0.018	749.468	5.594
*n*C17	13.572	22.674	21.333	13.304	2.304	0.719	8.147	9.425	9.83	6.030	2.767	1,032.367	4.305
*n*C18	12.874	21.677	20.607	12.443	3.802	0.682	7.789	9.010	9.50	5.640	4.566	1,041.270	5.390
*n*C19	10.535	21.434	20.233	15.074	3.634	0.558	7.702	8.909	9.32	6.832	4.36	1,279.023	4.650
*n*C20	9.359	16.853	16.331	9.943	3.737	0.496	6.056	7.005	7.53	4.507	4.488	1,120.536	7.428
*n*C21	6.793	16.126	15.045	9.457	3.229	0.360	5.794	6.703	6.93	4.286	3.878	1,509.044	3.430
*n*C22	5.757	13.167	12.343	8.366	3.258	0.305	4.731	5.473	5.69	3.792	3.913	1,450.221	3.924
*n*C23	4.752	10.261	9.259	6.302	2.372	0.252	3.687	4.265	4.27	2.856	2.849	1,363.579	0.036
D-C24		5.389	4.861	4.942	6.528		1.936	2.240	2.24	2.24	7.84		0.000
*n*C24	3.969	7.392	6.956	4.545	1.334	0.210	2.656	3.073	3.21	2.060	1.602	1,162.362	4.323
*n*C25	3.124	6.122	5.539	3.729	1.102	0.166	2.200	2.545	2.55	1.690	1.323	1,228.266	0.305
*n*C26	2.623	5.933	3.321	3.298		0.139	2.132	2.466	1.53	1.495	0	1,433.130	
*n*C27		3.72		1.885			1.337	1.546		0.854	0		
*n*C28		1.826		0.701			0.656	0.759		0.318	0		
Before *n*C8	1,334.078	185.257				70.722	66.566	77.004			0		
Before *n*C14	2,376.689	696.425	86.998	186.434		125.993	250.237	289.477	40.09	84.503	0		
Before toluene				52.553	43.952					23.820	24.696		